A Closed-Form Expression for Estimating the Maximum Radiated Emissions From a Heatsink on a Printed Circuit Board

Xinbo He, *Member, IEEE*, and Todd H. Hubing, *Fellow, IEEE*

***Abstract*—A closed-form expression is derived for determining the maximum possible radiated emissions from a heatsink over a printed circuit board or chassis plane as a function of the maximum voltage between the heatsink and plane. Two modes of radiation are considered: a patch-antenna mode and a monopole-antenna mode. The maximum emissions are the sum of the emissions due to each of these modes. Circuit board dimensions are assumed to be large compared to the heatsink dimensions. The most relevant parameters affecting the emissions are the dimensions of the heatsink. The closed-form expression is validated by comparing its results to full-wave simulation results for a variety of heatsink sizes and shapes.**

***Index Terms*—Electromagnetic modeling, electromagnetic radiation, maximum emissions.**

I. Introduction

ADVANCES in very large scale integration (VLSI) technology are producing faster and denser devices that often require large heatsinks to maintain allowable operating temperatures. These heatsinks are normally made of metal materials that can couple noise from the VLSI devices to the rest of the system.

At low frequencies where the heatsinks are much smaller than the shortest wavelength of the coupled noise, the heatsinks do not radiate electromagnetic energy efficiently. Usually, the only way for electrically small heatsinks to radiate enough to cause a radiated emissions problem is by coupling to larger structures such as conductive enclosures [1] or cables attached to the system [2], [3]. However, as operating frequencies get higher, heatsink dimensions can become comparable to, or even greater than, the noise wavelength. At these frequencies, heatsinks can radiate very efficiently [4]–[6]. In some situations, heatsinks can even serve as intentional antennas that perform dual functions: dissipating heat and communicating with electromagnetic waves [7], [8].

Manuscript received May 22, 2011; revised July 28, 2011; accepted September 14, 2011. Date of publication October 10, 2011; date of current version February 17, 2012. This work was supported in part by the National Science Foundation I/UCRC for Electromagnetic Compatibility.

X. He was with Clemson University, Clemson, SC 29634 USA. He is now with Apache Design Solutions, San Jose, CA 95134 USA (e-mail: xhe@clemson.edu).

T. H. Hubing is with Clemson University, Clemson, SC 29634 USA (e-mail: hubing@clemson.edu).

Color versions of one or more of the figures in this paper are available online at http://ieeexplore.ieee.org.

Digital Object Identifier 10.1109/TEMC.2011.2169248

In most cases, it is undesirable to have a heatsink geometry that radiates efficiently. Considerable research has been carried out on the influence that heatsink geometry can have on the radiated emissions from heatsinks [5], [9]–[11]. In earlier studies, the fin structure was ignored and only a conductive metal block was modeled to simplify simulations [4], [9]. More recently, the influence of the fins has been investigated, including fin length, height, spacing, orientation, and number of fins [12]–[14].

Several researchers have also investigated the mitigation of the unintentional emissions from heatsinks. The most common methods include the application of shorting posts, which connect the heatsink body to a nearby printed circuit board (PCB) ground [4], [5], [9], [15]. This method can work well for reducing the heatsink radiation at low frequencies. At least one report also investigates the use of conducting gaskets to electrically "cage" the IC, and thus reduces the radiated EMI [16].

In order to effectively squelch the radiated emissions from VLSI heatsinks, it is necessary to understand the radiation mechanism behind these emissions. Factors affecting heatsink radiation can include the heatsink dimensions, the proximity of the heatsink to the PCB ground, and properties of the noise source. However, there has not been a systematic study of how these factors affect the radiation from a VLSI heatsink above a circuit board.

Calculating the precise levels of radiated emissions from a heatsink in a complex system is neither practical nor desirable. Even if the precise nature of the VLSI components driving the heatsink could be determined, small variations in the heatsink geometry and its proximity to the board and other objects could have a profound influence on the radiated emissions at frequencies near resonance. In fact, at the frequencies of greatest interest (i.e., near resonance), the calculated field strengths would be the most susceptible to error. For this reason, engineers concerned with potential interference problems are usually not interested in determining the exact levels of radiated emissions for a precisely defined geometry. Instead, it is much more useful to obtain an accurate estimate of the maximum radiated emissions that is independent of small variations in the geometry or the influence of nearby components.

This paper presents a method for estimating the maximum possible radiated emissions for a heatsink with given maximum dimensions driven by a known voltage relative to a PCB. Although the voltage between a heatsink and a PCB is difficult to predict from pure simulations, it can be readily obtained by measurements of the VLSI component and is relatively

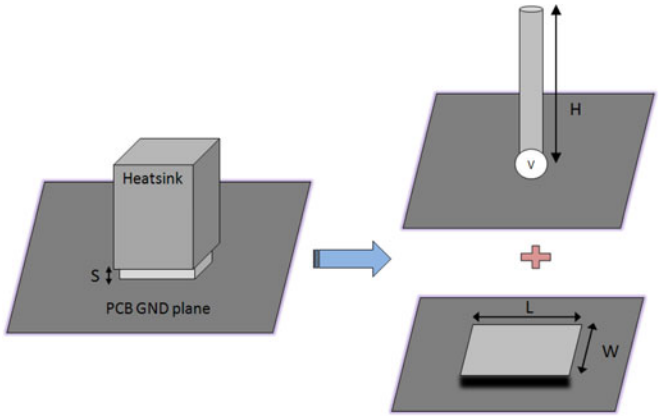

Fig. 1. Heatsink modeled as a superposition of a thick monopole and a patch antenna.

independent of the specific circuit board or heatsink geometry used for these measurements.

II. Model of a VLSI Heatsink

Radiation from a heatsink can be viewed as having two components: a cavity radiation component that dominates in short heatsinks with a large cross section and a monopole component that dominates when the heatsink is relatively tall [12], [17]. This concept is illustrated in Fig. 1. The cavity is the space between the heatsink bottom and the PCB plane. Normally, the spacing S between the heatsink body and the PCB ground plane is much smaller than the length L and width W of the heatsink bottom surface, and is much shorter than a wavelength at the frequencies of interest. Thus, the cavity can be modeled as a TM_z-2-D cavity where the electric field is constant in the vertical direction. The heatsink body can be modeled with good accuracy as a solid metal block if we are not interested in the small shifts in resonances caused by the fin structure [25]. When the heatsink is tall and thin above a relatively large PCB ground plane, it can be modeled as a thick monopole, which radiates effectively when its height H approaches a quarter wavelength.

When the radiated emissions from a system with a heatsink are evaluated, an important part of that evaluation is the characterization of the source. VLSI devices and their coupling to heatsinks can be difficult to model precisely. Depending on the software and the state of the device at any given time, the energy available to couple at a given frequency can vary widely. Nevertheless, it is possible to measure the voltages coupled to a heatsink by a VLSI device, and these measurements are relatively independent of the heatsink geometry [25]. Therefore, in this paper we start with an estimate or measurement of the maximum voltage between the heatsink and the plane and derive the maximum possible radiated emissions for that voltage.

III. Derivation of the Maximum Field to Voltage Ratio

In this section, a closed-form formula is derived to evaluate the maximum possible radiated emissions from a heatsink mounted above a PCB, when the maximum voltage around the cavity perimeter is known. The necessary input parameters are the physical dimensions of the heatsink and its spacing above the PCB. The formula is derived in two parts: maximum radiation from the heatsink cavity and maximum radiation from the heatsink as a monopole.

A. Patch-Antenna Component

At high frequencies (L or $W > \lambda/2$), the space between the heatsink and the PCB can behave like a cavity resonator. Other researchers have addressed the problem of calculating the maximum radiated emissions from a resonant 2-D cavity [18], [19]. These papers develop equations for obtaining the maximum voltage along the cavity walls when the source is well defined. The length L and the width W used in these equations must be extended to account for the edge effects. The extension is approximately twice the cavity height, which in this application is the spacing S between the heatsink and PCB [20], [21]. So,

$$L_{\mathrm{eff}} = L + 2S; \quad W_{\mathrm{eff}} = W + 2S \tag{1}$$

where L_{eff} and W_{eff} are the effective length and width of the cavity, respectively.

The equations derived in [18] and [19] are for a 2-D cavity formed by two identical plates. However, when the 2-D cavity is formed by a plate ($L_{\mathrm{eff}} \times W_{\mathrm{eff}}$) over a relatively large electrically conductive ground, the reflected E-field from the plane must be taken into account. For the purposes of estimating the maximum emissions, the PCB plane can be modeled as an infinite PEC ground. Thus, the maximum radiated E-field from such a cavity is twice the maximum field obtained in [18] and [19], or

$$|E|_{\max} = 2\frac{k\eta S I_{\mathrm{in}}}{4\pi r} = \frac{k\eta S I_{\mathrm{in}}}{2\pi r} \tag{2}$$

where k is the free space wavenumber, η is the free space intrinsic impedance, I_{in} is the maximum source current, and r is the observing distance.

The voltage along the edges of the cavity is approximately constant for any given frequency below the first resonance, and can be derived from the cavity transfer impedance formula [18], [19] as

$$|V|_{\max} = \frac{\eta S I_{\mathrm{in}}}{L_{\mathrm{eff}} W_{\mathrm{eff}} k}. \tag{3}$$

Thus, the $|E|_{\max}$ to $|V|_{\max}$ ratio is

$$\frac{|E|_{\max}}{|V|_{\max}} = \frac{k^2 L_{\mathrm{eff}} W_{\mathrm{eff}}}{2\pi r}. \tag{4}$$

For a resonating cavity, the far-field radiated emissions from the TM_{mn} ($m \neq 0$ and $n \neq 0$) are usually weaker than the nearby TM_{m0} ($m \neq 0$) or TM_{0n} ($n \neq 0$) modes [22], [23]. Thus, only the latter modes are considered. For frequencies above the first cavity resonance, the ratio can be obtained by calculating $|E|_{\max}$ from the far-field formula and obtaining $|V|_{\max}$ from the transfer impedance formula. For frequencies around the TM_{m0} modes of the cavity, the ratio is

$$\frac{|E_{m0}|_{\max}}{|V_{m0}|_{\max}} = \frac{mkW_{\mathrm{eff}}}{\pi r}. \tag{5}$$

Similarly for frequencies around the TM_{0n} modes, the ratio is

$$\frac{|E_{0n}|_{\max}}{|V_{0n}|_{\max}} = \frac{nkL_{\text{eff}}}{\pi r}. \tag{6}$$

By equating the low-frequency expression (4) to the high-frequency expression (5) at the first cavity resonance (TM_{10}), the connection point between the two expressions is

$$k_1 = \frac{2}{L_{\text{eff}}}. \tag{7}$$

For a normal cavity configuration without special structures that favor higher order TM_{m0} or TM_{0n} modes, the maximum radiated emissions will not exceed the emissions occurring at the TM_{01} mode [22]. So for frequencies above this mode, the maximum radiated emissions expression can be reduced to

$$\frac{|E|_{\max}}{|V|_{\max}} = \frac{|E_{01}|_{\max}}{|V_{01}|_{\max}} = \frac{k_{01}L_{\text{eff}}}{\pi r} = \frac{1}{r}\frac{L_{\text{eff}}}{W_{\text{eff}}} \tag{8}$$

where $k_{01} = 2\pi/2W_{\text{eff}}$ is the free space wavenumber at the TM_{01} resonance.

To allow for the possibility that the TM_{01} mode has a wide bandwidth, the connection frequency is shifted lower by averaging the resonant frequencies of the TM_{01} mode and the highest TM_{m0} mode, which is no higher than the TM_{01} mode [22]. The revised connection frequency is then given by

$$k = \left(\frac{\pi}{W_{\text{eff}}} + \frac{\pi p}{L_{\text{eff}}}\right)/2 \tag{9}$$

where p is $L_{\text{eff}}/W_{\text{eff}}$ rounded to the nearest integer.

The formula for the maximum cavity radiation is then

$$\left.\frac{|E|_{\max}}{|V|_{\max}}\right|_{\text{Patch}} = \begin{cases} \dfrac{k^2 L_{\text{eff}} W_{\text{eff}}}{2\pi r}, & k \le \dfrac{2}{L_{\text{eff}}} \\ \dfrac{kW_{\text{eff}}}{\pi r}, & \dfrac{2}{L_{\text{eff}}} < k \le \left(\dfrac{\pi}{W_{\text{eff}}} + \dfrac{\pi p}{L_{\text{eff}}}\right)\Big/2 \\ \dfrac{L_{\text{eff}}}{rW_{\text{eff}}}, & k > \left(\dfrac{\pi}{W_{\text{eff}}} + \dfrac{\pi p}{L_{\text{eff}}}\right)\Big/2. \end{cases} \tag{10}$$

B. Monopole-Antenna Component

The heatsink body can be modeled as a thick monopole when the heatsink is taller than its width. The radiated emissions from a monopole are well known. The expression for the maximum radiated field from a monopole at its first resonance is [23]

$$E_{\max} = \frac{\eta_o I_o}{2\pi r}, \quad \text{at } \theta = \frac{\pi}{2} \tag{11}$$

where I_o is the source current of the monopole antenna.

$|E|_{\max}$ in (11) is derived from the first resonance of the monopole. For frequencies higher than the first resonance, an ideal monopole's maximum radiated field can be higher than it is at the first resonance. However, these higher levels of radiated emissions only occur in narrow lobes for thin, low-loss antennas and this equation works well even at high frequencies for realistic heatsink dimensions. Thus, (11) is used to represent the maximum emissions due to monopole radiation at all frequencies.

The maximum voltage at the monopole input at resonance is $V_{\max} = I_o \times R_{\text{res}}$, where R_{res} is the resonant input resistance of the monopole. Thus, the ratio of the maximum radiated electric field to the maximum voltage at the feed port for the resonant monopole is

$$\frac{|E|_{\max}}{|V|_{\max}} = \frac{\eta_o}{2\pi r R_{\text{res}}} = \frac{120\pi}{2\pi r R_{\text{res}}} = \frac{60}{rR_{\text{res}}}. \tag{12}$$

At frequencies lower than the first monopole resonance, the input impedance is mostly capacitive and thus approximately inversely proportional to frequency. So the feed voltage to this thick monopole is also inversely proportional to frequency if the feed current is constant. At the same time, the maximum radiated field is proportional to frequency for a short (shorter than a quarter wavelength) monopole with a constant feed current [23]. Thus, the ratio of $|E|_{\max}$ to $|V|_{\max}$ is approximately proportional to the square of the frequency, and can be written as

$$\frac{|E|_{\max}}{|V|_{\max}} \approx \left(\frac{f}{f_{1\text{st}}}\right)^2 \frac{60}{rR_{\text{res}}} \tag{13}$$

where $f_{1\text{st}}$ is the first resonant frequency of the thick monopole, and f is no higher than $f_{1\text{st}}$.

The first monopole resonance occurs when the heatsink is approximately one quarter-wavelength tall. Expressions for the input impedance of a monopole at resonance are available in the literature (e.g., [23]) and simulations by the authors [25] indicate that the minimum input resistance of an antenna radiating like a monopole at resonance is approximately 36–40 Ω regardless of the specific dimensions of the antenna. Setting R_{res} to 36 Ω in (13) provides an equation for the maximum possible radiated emissions (at frequencies up to the first resonance) from a heatsink radiating like a monopole at a given distance and for a given input voltage.

The first resonant frequency of a monopole occurs when its height approaches a quarter wavelength. However, for a thick monopole where the dimensions of the end face are not negligible, the first resonant frequency is shifted lower. The additional distance that current flows across the end surfaces can be viewed as increasing the effective length of a fat monopole. An approximation of the shifted resonant frequency is then

$$f_{1\text{st-shifted}} = \frac{c_o}{4\left(H + S + \sqrt{L_{\text{eff}}^2 + W_{\text{eff}}^2}/2\right)} \tag{14}$$

where c_o is the speed of light in free space. This approximation was verified with full-wave simulations in [25].

So, the final expression for the monopole component of the heatsink radiated field is

$$\left.\frac{|E|_{\max}}{|V|_{\max}}\right|_{\text{Monopole}} = \begin{cases} \left(\dfrac{f}{f_{1\text{st-shifted}}}\right)^2 \dfrac{60}{rR_{\text{res}}}, & f < f_{1\text{st-shifted}} \\ \dfrac{60}{rR_{\text{res}}}, & f \ge f_{1\text{st-shifted}}. \end{cases} \tag{15}$$

C. Maximum Emissions Estimate

When combining the maximum electric field contributions of the cavity and the heatsink body, (10) and (15) are separately calculated and then added

$$\left.\frac{|E|_{\max}}{|V|_{\max}}\right|_{\text{Heatsink}} = \left.\frac{|E|_{\max}}{|V|_{\max}}\right|_{\text{Patch}} + \left.\frac{|E|_{\max}}{|V|_{\max}}\right|_{\text{Monopole}}. \quad (16)$$

The added results overestimate the radiated emissions in most cases. However, the overestimation is minimal when both components are significant and coincident.

The final formula for the maximum radiated field can be written in the following segmented form (17a)–(17c), as shown at the bottom of this page, where $k_{\text{hs}} = 2\pi f_{\text{1st-shifted}}/c_o$ is the free space wavenumber for the thick monopole's first resonance.

IV. Model Validation

To validate the closed-form expression (17), several heatsink configurations were evaluated using a full-wave field solver [24] and the results were compared to (17). An initial heatsink with size ($L = 90$ mm, $W = 64$ mm, $S = 6$ mm, and $H = 38$ mm) [15] was evaluated. Then, its height was varied from 0 mm to 600 mm. At very small heights, the heatsink resembled a patch antenna. When the height was much larger than L and W, the heatsink looked more like a monopole antenna.

Multiple sources were used in one heatsink configuration to demonstrate that (17) applies regardless of the number of independent sources driving the heatsink or the location of these sources. For each configuration evaluated, the full-wave simulation results and the ratios obtained from (17) are plotted in the same figure for comparison.

Fig. 2 shows both the maximum emissions estimate and the actual emissions obtained from a full-wave [24] simulation of a heatsink with negligible height driven by an ideal current source located close to the center. Since the zero-height heatsink is essentially a patch antenna, it is not surprising that the actual emission peaks come very close to the maximum emissions estimate at several frequencies.

When the heatsink height is increased to 5 or 38 mm (see Figs. 3 and 4, respectively), both the estimation and the full-wave field strengths increase, though these heatsinks are still relatively short compared to their cross sections. In these cases,

$$\frac{|E|_{\max}}{|V|_{\max}} = \begin{cases} \dfrac{k^2 L_{\text{eff}} W_{\text{eff}}}{2\pi r} + \left(\dfrac{k}{k_{\text{hs}}}\right)^2 \dfrac{60}{rR_{\text{res}}} & k \le k_{\text{hs}} \\ \dfrac{k^2 L_{\text{eff}} W_{\text{eff}}}{2\pi r} + \dfrac{60}{rR_{\text{res}}} & k_{\text{hs}} < k \le \dfrac{2}{L_{\text{eff}}} \\ \dfrac{kW_{\text{eff}}}{\pi r} + \dfrac{60}{rR_{\text{res}}} & \dfrac{2}{L_{\text{eff}}} < k \le \left(\dfrac{\pi}{W_{\text{eff}}} + \dfrac{\pi p}{L_{\text{eff}}}\right)\Big/2 \\ \dfrac{L_{\text{eff}}}{rW_{\text{eff}}} + \dfrac{60}{rR_{\text{res}}} & k > \left(\dfrac{\pi}{W_{\text{eff}}} + \dfrac{\pi p}{L_{\text{eff}}}\right)\Big/2 \end{cases} \quad k_{hs} \le \frac{2}{L_{\text{eff}}} \quad (17a)$$

$$\frac{|E|_{\max}}{|V|_{\max}} = \begin{cases} \dfrac{k^2 L_{\text{eff}} W_{\text{eff}}}{2\pi r} + \left(\dfrac{k}{k_{\text{hs}}}\right)^2 \dfrac{60}{rR_{\text{res}}} & k \le \dfrac{2}{L_{\text{eff}}} \\ \dfrac{kW_{\text{eff}}}{\pi r} + \left(\dfrac{k}{k_{\text{hs}}}\right)^2 \dfrac{60}{rR_{\text{res}}} & \dfrac{2}{L_{\text{eff}}} < k \le k_{\text{hs}} \\ \dfrac{kW_{\text{eff}}}{\pi r} + \dfrac{60}{rR_{\text{res}}} & k_{\text{hs}} < k \le \left(\dfrac{\pi}{W_{\text{eff}}} + \dfrac{\pi p}{L_{\text{eff}}}\right)\Big/2 \\ \dfrac{L_{\text{eff}}}{rW_{\text{eff}}} + \dfrac{60}{rR_{\text{res}}} & k > \left(\dfrac{\pi}{W_{\text{eff}}} + \dfrac{\pi p}{L_{\text{eff}}}\right)\Big/2 \end{cases} \quad \frac{2}{L_{\text{eff}}} < k_{\text{hs}} \le \left(\frac{\pi}{W_{\text{eff}}} + \frac{\pi p}{L_{\text{eff}}}\right)\Big/2 \quad (17b)$$

$$\frac{|E|_{\max}}{|V|_{\max}} = \begin{cases} \dfrac{k^2 L_{\text{eff}} W_{\text{eff}}}{2\pi r} + \left(\dfrac{k}{k_{\text{hs}}}\right)^2 \dfrac{60}{rR_{\text{res}}} & k \le \dfrac{2}{L_{\text{eff}}} \\ \dfrac{kW_{\text{eff}}}{\pi r} + \left(\dfrac{k}{k_{\text{hs}}}\right)^2 \dfrac{60}{rR_{\text{res}}} & \dfrac{2}{L_{\text{eff}}} < k \le \left(\dfrac{\pi}{W_{\text{eff}}} + \dfrac{\pi p}{L_{\text{eff}}}\right)\Big/2 \\ \dfrac{L_{\text{eff}}}{rW_{\text{eff}}} + \left(\dfrac{k}{k_{\text{hs}}}\right)^2 \dfrac{60}{rR_{\text{res}}} & \left(\dfrac{\pi}{W_{\text{eff}}} + \dfrac{\pi p}{L_{\text{eff}}}\right)\Big/2 < k \le k_{\text{hs}} \\ \dfrac{L_{\text{eff}}}{rW_{\text{eff}}} + \dfrac{60}{rR_{\text{res}}} & k > k_{\text{hs}} \end{cases} \quad k_{\text{hs}} > \left(\frac{\pi}{W_{\text{eff}}} + \frac{\pi p}{L_{\text{eff}}}\right)\Big/2 \quad (17c)$$

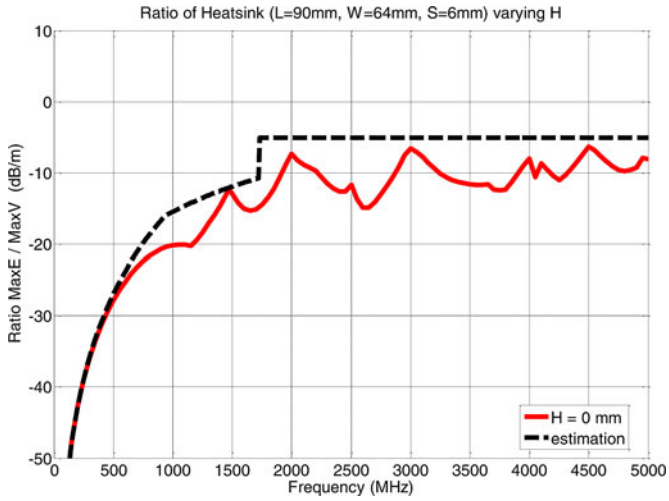

Fig. 2. Field-to-voltage ratio for a 90 mm × 64 mm × 0 mm heatsink 6 mm above a plane.

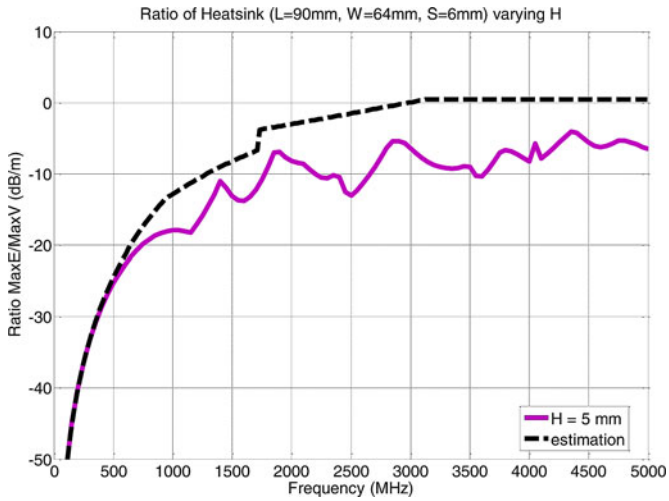

Fig. 3. Field-to-voltage ratio for a 90 mm × 64 mm × 5 mm heatsink 6 mm above a plane.

the overestimation is larger. This larger difference is the result of directly adding the maximum radiated fields from both components, whose direction of maximum radiation occurs at different spatial positions and/or different frequencies.

As the height is further increased to 76 mm (see Fig. 5), the first resonance of the monopole shows up. This resonance occurs at about 515 MHz as predicted by (14).

As the heatsink height continues to increase to 150 and 600 mm (see Figs. 6 and 7, respectively), the height becomes larger than the other dimensions and the resonances of the monopole component show up at frequencies much lower than the first cavity resonance. The actual emission levels are close to the estimate at these resonance peaks.

The previous simulation results used only one excitation source. In real situations, multiple sources could exist and independently drive the heatsink. To evaluate this possibility, multiple independent sources were used to drive one of the heatsink configurations and the results are compared to (17) in Fig. 8.

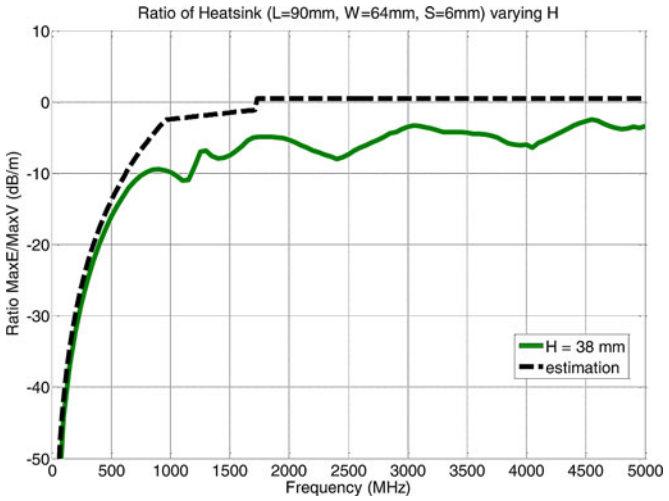

Fig. 4. Field-to-voltage ratio for a 90 mm × 64 mm × 38 mm heatsink 6 mm above a plane.

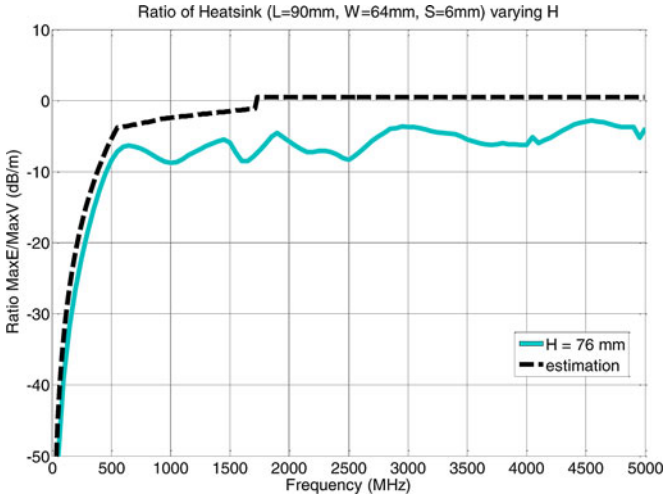

Fig. 5. Field-to-voltage ratio for a 90 mm × 64 mm × 76 mm heatsink 6 mm above a plane.

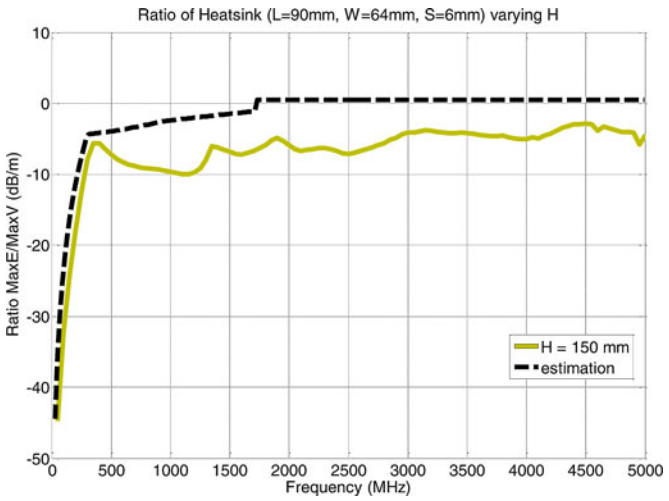

Fig. 6. Field-to-voltage ratio for a 90 mm × 64 mm × 150 mm heatsink 6 mm above a plane.

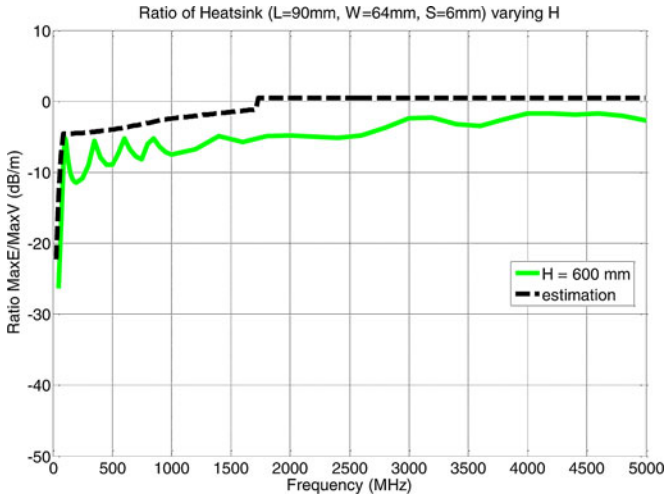

Fig. 7. Field-to-voltage ratio for a 90 mm × 64 mm × 600 mm heatsink 6 mm above a plane.

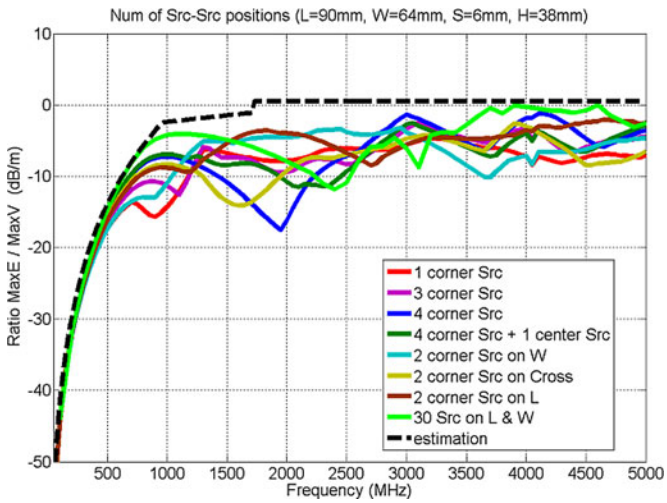

Fig. 8. Field-to-voltage ratio for a 90 mm × 64 mm × 38 mm heatsink 6 mm above a plane driven by sources at various locations.

For multiple independent sources, even for up to 30 sources distributed around the cavity edges, the estimate provides a good envelope.

In addition to the results shown here, the authors have evaluated many additional heatsink geometries of different sizes and cross sections and have yet to observe radiated emissions higher than predicted by the maximum emissions estimate obtained by (17) [25].

V. Conclusion

A maximum emissions estimate for heatsink-PCB configurations has been derived by viewing the radiation source as being a combination of monopole and resonant-patch antennas. The estimate relates the maximum possible radiated emissions to the maximum voltage between the heatsink and the circuit board. Maximum emissions estimates like this can be used to determine whether a particular source-antenna structure might possibly cause a radiated emissions problem. The only parameters required for this estimate are the dimensions of the heatsink and the maximum applied voltage. This expression has been shown to be effective for various heatsink dimensions, including short, fat heatsinks and tall, thin heatsinks.

References

[1] M. Li, J. Drewniak, S. Radu, J. Nuebel, T. Hubing, R. DuBroff, and T. Van Doren, "An EMI estimate for shielding-enclosure evaluation," *IEEE Trans. Electromag. Compat.*, vol. 43, no. 3, pp. 295–304, Aug. 2001.

[2] H. W. Shim and T. H. Hubing, "Model for estimating radiated emissions from a printed circuit board with attached cables driven by voltage-driven sources," *IEEE Trans. Electromag. Compat.*, vol. 47, no. 4, pp. 899–907, Nov. 2005.

[3] S. Deng, T. Hubing, and D. Beetner, "Characterizing the electric-field coupling from IC-heatsink structures to external cables using TEM-cell measurements," *IEEE Trans. Electromagn. Compat.*, vol. 49, no. 4, pp. 785–791, Nov. 2007.

[4] C. F. Lee, K. Li, S. Y. Poh, R. T. Shin, and J. A. Kong, "Electromagnetic radiation from a VLSI package and heatsink configuration," in *Proc. 1991 IEEE Int. Symp. Electromagn. Compat.*, Aug., pp. 393–398.

[5] C. E. Brench, "Heatsink radiation as a function of geometry," in *Proc. 1994 IEEE Int. Symp. Electromagn. Compat.*, 1994, pp. 105–109.

[6] D. Moongilan, "Radiated emissions from proximity coupled oversized heat-sinks," in *Proc. 2007 IEEE Int. Symp. Electromagn. Compat.*, Honolulu, HI, Jul. 2007, pp. 1–6.

[7] L. Covert and J. Lin, "Simulation and measurement of a heat sink antenna: A dual function structure," *IEEE Trans. Antennas Propag.*, vol. 54, no. 4, pp. 1342–1349, Apr. 2006.

[8] A. Alnukari, P. Guillemet, Y. Scudeller, and S. Toutain, "Active heatsink antenna for radio-frequency transmitter," *IEEE Trans. Adv. Packag.*, vol. 33, no. 1, pp. 139–146, Feb. 2010.

[9] K. Li, C. F. Lee, S. Y. Poh, R. T. Shin, and J. A. Kong, "Application of FDTD method to analysis of electromagnetic radiation from VLSI heatsink configurations," *IEEE Trans. Electromagn. Compat.*, vol. 35, no. 2, pp. 204–214, 1993.

[10] N. J. Ryan, D. A. Stone, and B. Chambers, "FDTD modeling of heatsinks for EMC," in *Proc. Int. Conf. and Exhib. Electromagnetic Compatibility*, Jul. 1999, pp. 125–130.

[11] N. J. Ryan, B. Chambers, and D. A. Stone, "FDTD modeling of heatsink RF characteristics for EMC mitigation," *IEEE Trans. Electromagn. Compat.*, vol. 44, no. 3, pp. 458–465, Aug. 2002.

[12] S. K. Das and T. Roy, "An investigation of radiated emissions from heatsinks," in *Proc. 1998 IEEE Symp. Electromagn. Compat.*, vol. 2, pp. 784–789.

[13] J. Nonaka, S. Nitta, A. Mutoh, and T. Miyashita, "The influence of straight-fin heatsink on noise susceptibility of IC-capacitive coupling," in *Proc. 1999 IEEE Int. Symp. Electromagn. Compat.*, no. 1, pp. 345–350.

[14] P. Qu, M. K. Iyer, and Y. Qiu, "Radiated emission from pin-fin heat sink mounted on an EBGA package," in *Proc. Electr. Perform. Electron. Packag.*, 1999, pp. 199–202.

[15] B. Archambeault, J. Chen, S. Pratepeni, L. Zhang, and D. Wittwer, "Comparison of various numerical modeling tools against a standard problem concerning heat sink emissions—Standard Modeling Paper 3," IEEE EMC Society TC9. [Online]. Available: http://www.ewh.ieee.org/cmte/tc9/

[16] J. C. Diepenbrock, B. Archambeault, and L. D. Hobgood, "Improved grounding method for heat sinks of high speed processors," in *Proc. Electron. Compon. Technol. Conf.*, 2001, vol. 51, pp. 993–996.

[17] D. Hockanson and R. D. Slone, "Investigation of EMI coupling at CPU interconnect," in *Proc. 2004 IEEE Int. Symp. Electromagn. Compat.*, Aug., vol. 2, pp. 424–429.

[18] H. Shim and T. Hubing, "A closed-form expression for estimating radiated emissions from the power planes in a populated printed circuit board," *IEEE Trans. Electromagn. Compat.*, vol. 48, no. 1, pp. 74–81, Feb. 2006.

[19] M. Leone, "The radiation of a rectangular power-bus structure at multiple cavity-mode resonances," *IEEE Trans. Electromagn. Compat.*, vol. 45, no. 3, pp. 486–492, Aug. 2003.

[20] P. Bhartia, I. Bahl, R. Garg, and A. Ittipiboon, *Microstrip Antenna Design Handbook*. Norwood, MA: Artech House, Nov. 2000.

[21] K. P. Ray and G. Kumar, "Determination of the resonant frequency of microstrip antennas," *Microw. Opt. Technol. Lett.*, vol. 23, no. 2, pp. 114–117.

[22] H. Zeng, H. Ke, G. Burbui, and T. Hubing, "Determining the maximum allowable power bus voltage to ensure compliance with a given radiated emissions specification," *IEEE Trans. Electromagn. Compat.*, vol. 51, no. 3, p. 868-872, Aug. 2009.
[23] C. A. Balanis, *Antenna Theory: Analysis and Design*, 3rd ed. New York: Wiley-Interscience, Apr. 2005.
[24] Y. Ji and T. Hubing, "EMAP5: A 3D Hybrid FEM/MOM code," *J. Appl. Comput. Electromagn. Soc.*, vol. 15, no. 1, pp. 1–12, Mar. 2000.
[25] X. He and T. Hubing, "Special considerations for PCB heatsink radiation estimation," Clemson Veh. Electron. Lab., Greenville, SC, Tech. Rep. CVEL-11-027, Apr. 2011.

Xinbo He (S'08) received the B.Eng. degree from Xian Jiaotong University, Xian, China, and Master's degrees from Xian Jiaotong University, National University of Singapore, Singapore, and University of Missouri-Rolla, Rolla, in 1997, 2000, and 2006, respectively. In 2011, he received the Ph.D. degree in electrical engineering from Clemson University Clemson, SC.

From 2001 to 2004, he worked as a Senior Research Officer at Institute of Materials Research and Engineering, Singapore. He is currently an Engineer with Apache Design Solutions, San Jose, CA. His current research interests include electromagnetic modeling and computational electromagnetics.

Todd H. Hubing (S'82–M'82–SM'93–F'06) received the B.S.E.E. degree from the Massachusetts Institute of Technology, Cambridge, in 1980, the M.S.E.E. degree from Purdue University, IN, in 1982, and the Ph.D. degree in electrical engineering from North Carolina State University, Raleigh, in 1988.

From 1982 to 1989, he was with the Electromagnetic Compatibility Laboratory, IBM Communications Products Division, Research Triangle Park, NC. In 1989, he became a faculty member at the University of Missouri-Rolla (UMR) where he worked with other faculty and students to analyze and develop solutions for a wide range of EMC problems affecting the electronics industry. In 2006, he joined Clemson University, Clemson, SC, as the Michelin Professor for vehicle electronic systems integration, where he is involved in research on electromagnetic compatibility and computational electromagnetic modeling, particularly as it is applied to automotive and aerospace electronics.

Dr. Hubing was the President of the IEEE Electromagnetic Compatibility Society and currently serves on the society's board of directors. He is a Fellow of the Applied Computational Electromagnetic Society.